

THE INTERMEDIATE LINE REGION IN AGN: A REGION “PRÆTER NECESSITATEM”?

J. W. Sulentic¹ and P. Marziani²

Subject headings: Galaxies: Seyfert – Galaxies: Emission Lines – Galaxies: Quasars – Line: Formation – Line: Profiles

ABSTRACT

As a consequence of improved S/N, spectral resolution and wavelength coverage various authors have introduced, without strong justification, new emitting regions to account for various emission line profile differences in AGN. The so-called CIV λ 1549 intermediate line region (ILR) appears to be especially ill-defined. We present observational evidence that suggests the ILR is statistically indistinguishable from the classical narrow line region (NLR). We present the results of theoretical models showing that a smooth density gradient in the NLR can produce CIV and Balmer emission lines with different widths. The putative ILR component has often been included with the broad line profile in studies of CIV BLR properties. Failure to account for the composite nature of CIV emission, and for the presence of sometimes appreciable NLR CIV emission, has important consequences for our understanding of the BLR.

¹Department of Physics and Astronomy, University of Alabama, Tuscaloosa, AL 35487; giacomo@merlot.astr.ua.edu

²Osservatorio Astronomico di Padova, vicolo dell’Osservatorio 5, I-35122 Padova, Italy; marziani@pd.astro.it

1. Introduction

Observed profiles of different emission lines often show intriguing differences in width and relative velocity. In some objects, there is a rather strong correlation between line width and critical density or ionization potential (De Robertis & Osterbrock 1986). These trends have led to the concept of a density gradient across the line emitting regions, with the higher critical density (or higher ionization) lines being emitted closer to the continuum source. The underlying assumption is that the velocity dispersion decreases with increasing distance from the source of ionizing photons, as expected for gas whose motion is predominantly rotational or virialized. Variations in line width complicate attempts to separate the broad (BLR) and narrow (NLR) line contributions in a source. The frequent observation of a prominent component with $\text{FWHM} \sim 1600 \text{ km s}^{-1}$ in the $\text{CIV} \lambda 1549$ (hereafter CIV) profile complicates the interpretation of high ionization line (HIL) properties in particular. In an attempt to take into account the diverse widths of emission lines, some workers have proposed the existence of an "Intermediate Line Region" (ILR) (see e.g. Wills et al. 1993). This emission component has been routinely treated as part of the BLR emission in line profile studies either: a) because it is believed to be part of the non-NLR gas or b) because a clear inflection between the emitting components is not often seen in the CIV profile making it difficult to subtract (see e.g. Baldwin 1997, p. 92).

In Section 2 we discuss three observational results: 1) an unambiguous CIV NLR component with FWHM similar to $[\text{OIII}] \lambda 5007$ is seen in many Seyfert 2 galaxies, 2) a similar component is also identified in some broad line AGN (with and without an inflection) although the component is often broader with mean $\text{FWHM} \sim 900 \text{ km s}^{-1}$ broader than $\text{FWHM H}\beta$ ($\approx \text{FWHM } [\text{OIII}] \lambda 5007$) and 3) except for the broader profile width the "narrower" CIV component shows properties very similar to those ascribed to the classical NLR. Section 3 presents model calculations to show that the diversity of narrow line profile widths can be ascribed to a smooth gradient of physical properties in the NLR, and that a larger width, $\sim 1000-2000 \text{ km s}^{-1}$, is expected for CIV without invoking a new (ILR) emitting region. Finally, in Section 4 we argue: a) that introduction of a new emitting region is unjustified and b) that BLR properties inferred from

the CIV line are strongly dependent on whether or not a narrow component is subtracted.

2. An Unambiguous CIV NLR is Observed in Some AGN

Most of the UV spectroscopic data for Seyfert 2 sources comes from the IUE archive. While the resolution of this data is limited, it shows that the majority of Seyfert 2 galaxies exhibit a narrow line component of CIV. We assume, following unification ideas, that BLR CIV and $\text{H}\beta$ are obscured in Seyfert 2's and that we see only NLR emission, the same NLR in Seyfert 1 and 2 sources. Study of averaged spectra for a sample of twenty mostly "pure" Seyfert 2 sources (Heckmann et al. 1995) show a significant narrow CIV line. Detailed study of IUE spectra for NGC 7674 and I Zw 92 (Kraemer et al. 1994) show an NLR line intensity ratio $\text{CIV}/\text{H}\beta \approx 2.0$. NGC 1068 and 5643 are the only Seyfert 2 sources in the HST archive with high s/n FOS spectra of the CIV region. NGC 1068 is the brightest example of a Seyfert 2 with a confirmed hidden BLR (Antonucci & Miller 1985). Recent study of the FOS spectra for NGC 1068 (Kraemer, Ruiz & Crenshaw 1998) show that it contains a strong $\text{CIV} \lambda 1549$ NLR component (partially resolved into $\lambda \lambda 1548/1551$ components) with $\text{FWHM} \approx 1100 \pm 200 \text{ km s}^{-1}$. The narrow component of $\text{H}\beta$, and $[\text{OIII}] \lambda 5007$ show profile $\text{FWHM} \approx 1000 \pm 200 \text{ km s}^{-1}$ (Caganoff et al. 1991). Clear evidence for NLR CIV ($\text{FWHM} = 1180 \text{ km s}^{-1}$) is also seen in a bright Seyfert 1.5 galaxy, NGC 5548 (Goad & Koratkar 1998). The NLR component in NGC 5548 remained constant while the BLR component went through large changes, reenforcing the idea that independent NLR and BLR components exist in that source.

The above cited observations make it clear that NLR CIV exists in many lower luminosity AGN. It is unambiguous in Seyfert 2 sources but can be very confusing in sources that show BLR emission because a clear NLR/BLR profile inflection is only occasionally observed. It has been argued (Wills et al. 1993) that higher luminosity sources do not show an NLR component. This argument arose from profile analysis of a small sample of high luminosity radio loud sources (Wills et al. 1993). The NLR was concluded to be weak or absent in these sources because no significant profile component that matched the width of $[\text{OIII}] \lambda 5007$ was found. This interpretation was

widely accepted, in part, because reddening was assumed to be high in the NLR ($E(B-V) \sim 0.5$). The above cited data suggests: 1) that the reddening is frequently not so high (Kraemer, Ruiz & Crenshaw 1998 derive a nuclear reddening of only $E(B-V) = 0.02$ for NGC1068) and/or 2) that CIV is amplified by some physical process (see section 3). The current interpretation of narrow line spectra in NGC 1068 and 5548 points toward relatively high density and ionization parameter at the inner edge of the NLR. A value of $\Gamma \sim 10^{-1.5}$ accounts for the strength of several high ionization lines (Kraemer et al. 1998). The dereddened NLR intensity ratio $CIV\lambda 1549/H\beta$ is ≈ 14 for NGC 5548, and an inner NLR component with $CIV\lambda 1549/H\beta \approx 30$ appears to be necessary. Recently, Ferguson et al. (1997) interpreted the strength of the strongest coronal lines observed in the spectra of Seyfert galaxies in terms of emission from photoionized gas in a rather dense region which could also be associated with the innermost NLR.

Our own line profile survey (Marziani et al. 1996: MS) of a heterogeneous sample of 52 AGN found examples of both high and low luminosity sources with a narrow CIV component comparable in width to $[OIII]\lambda 5007$. However a considerable number of sources showed a narrow component of CIV (and $[OIII]\lambda 4363$, when it could be resolved from $H\gamma$) that was broader than $[OIII]\lambda 5007$ by as much as 1500 km s^{-1} . Figure 1 illustrates the distributions of broad and narrow line widths found for CIV and $H\beta$ in the MS survey. The simplest interpretation is that both CIV NLR and BLR are broader than the corresponding regions in $H\beta$. Additional support for our NLR interpretation of the narrower CIV component comes from observations of sources where the NLR is resolved. In the case of the Seyfert 2 galaxy NGC 5643, the CIV NLR feature is obviously broader, even in the extended emission line region (EELR: $\text{FWHM} = 1800 \pm 200 \text{ km s}^{-1}$), than either NLR $\text{HeII}\lambda 1640$ or NLR $CIII]\lambda 1909$. PG2308+098 is an example of a higher luminosity ($z=0.43$) source from the MS survey that shows a clear inflection between the broad and, one of the broadest observed, narrow CIV components. We derived a $\text{FWHM} \approx 2630 \text{ km s}^{-1}$ for the narrow CIV component considerably broader than $\text{FWHM} \approx 700 \pm 100 \text{ km s}^{-1}$ measured for $H\beta$ and $[OIII]\lambda 5007$ in that source. Figure 2 shows a comparison between the CIV feature in the NGC 5643 EELR and the narrow CIV component derived for PG 2308+098. Figure 2 clearly shows

that the width of the two narrow features are equal within the observational errors. Narrow component widths as broad as the one observed in PG2308+098 are clearly not unprecedented in unambiguous NLR emitting regions.

3. NLR Models: A Broader and Stronger $CIV\lambda 1549$ Line

We calculated photoionization models of the NLR and computed the emergent spectrum using CLOUDY (Ferland 1996). Our goal was to account for FWHM differences as large as $\Delta v_r \lesssim 2000 \text{ km s}^{-1}$ (mean difference $\Delta V = 900 \text{ km s}^{-1}$) between $H\beta$ and CIV. We did not attempt sophisticated model innovations nor did we try to fit the line profiles of a particular source. We attempted instead to illustrate the implications of recent robust results involving the input to photoionization calculations for the $CIV\lambda 1549$ and $H\beta$ line profiles when the NLR line emission is not spatially resolved (presently the case for the vast majority of AGN). At $z \approx 0.2$, a $0.^{\circ}25$ aperture (typically employed for FOS observations) covers 1 kpc of spatial extent: thus most of the NLR should be included in a measurement.

Input parameters for our models are listed in Table 1. We assumed spherical symmetry with a radial density gradient described by a power-law, $n_e = n_0 r_{pc}^{-s}$ cm^{-3} from $1-10^3$ pc. The density at the outer edge of the NLR was set equal to 10^3 cm^{-3} in all cases. We assumed a power-law dependence for the covering factor, i. e. $f_{c,r} \propto r^{-m}$, with total NLR covering factor 0.1. The first three models listed in Table 1 follow Netzer (1990) with a column density $N_c \propto r^{-2/3s}$. The last four models assumed that $N_c \approx 10^{23} \text{ cm}^{-2} = \text{constant}$ throughout the NLR (Column 3 lists adopted values of m). The inclusion of the effects of appreciable mechanical heating appear to be necessary for realistic modeling of the NLR. HST narrow-band images and radio maps have show a close relationship between radio ejecta and NLR emitting plasma in several nearby Seyfert galaxies (Capetti et al. 1999; Falcke et al. 1998). A crude estimate of the heating rate ϵ can be obtained by assuming that a fraction $f_p \approx 0.1$ (approximately equal to the covering factor f_c) of the jet energy flux Π is converted into heating of the NLR gas. Assuming an exponential radial dependence of the heating rate we can write $\epsilon = \epsilon_0 f_{c,0.1} R_{out,1kpc}^{-3} \Pi_{45} \exp(-(r - r_0)/r_s) \text{ ergs s}^{-1} \text{ cm}^{-3}$, where we have parameterized the depen-

dence on outer radius (R_{out}), f_c , and Π (Column 4 lists the scale factor). The values $r_s = 1$ and 10pc correspond, respectively, to a heating rate per unit volume at 1 pc $\log \epsilon_0 \approx -9.38$ (which is negligible) and ≈ -6.37 (which provides significant enhancement of electron temperature, in a cocoon within 2 pc). The latter cases is also more realistic because recent hydrodynamic simulations show that most of the line luminosity is concentrated in dense clouds surrounding the jet (Steffen et al. 1997). However, recent observations (Villar-Martin et al. 1999) of high redshift radio-loud and quiet sources reveal $\text{FWHM} \gtrsim 1000\text{ km s}^{-1}$ emission lines in extended gas both near and far from radio jets. The jet energy flux is a poorly known quantity, and its actual relevance depends on the details of the jet/cloud interaction. Significant heating of clouds can however be expected for a wide range of AGN including radio quiet objects like Seyferts (in agreement with the analysis of Bicknell et al. 1998 for Seyfert 2 galaxies).

The gas is assumed to move with velocity $v(r) = (2100r^{-1/2} + 0.1r)$ i.e., at the local virial velocity plus a component due to galactic rotation. A velocity dispersion $\Delta v \approx 4150r_1^{-0.5}\text{pc}M_9^{0.5}\text{ km s}^{-1}$ is expected at a distance r equal to 1 pc (which we assume as the inner edge of the NLR; $1\text{ pc} \approx 10^4$ gravitational radii for a $10^9 M_\odot$ black hole), if the gas motion is rotational or virial. We focus our profile predictions on four NLR lines: CIV, H β , [OIII] $\lambda 5007$, and [Fe VII] $\lambda 6087$. The widths reported in Table 1 (Cols. 5–8) are the weighted average of velocity over line emissivity per unit area ζ_r (i.e., $\langle v \rangle = \int v_r f_{c,r} \zeta_r dV / \int f_{c,r} \zeta_r dV$). Observed NLR linewidth for [OIII] $\lambda 5007$, H β , and [Fe VII] $\lambda 6087$ are reproduced by the models ($\text{FWHM}([\text{OIII}]\lambda 5007) \approx \text{FWHM}(\text{H}\beta) < \text{FWHM}([\text{Fe VII}]\lambda 6087) \sim 1000\text{ km s}^{-1}$), with models 5 and 7 a slightly larger with of [OIII] $\lambda 5007$ with respect to H β , as it is often observed. The most relevant result is that $\langle v \rangle$ for CIV $\lambda 1549$ appears to be significantly larger than that of any other line considered, with $\langle v \rangle \sim 1000 - 2500\text{ km s}^{-1} \gtrsim 1000\text{ km s}^{-1}$ in all cases. CIV $\lambda 1549$ emission is favored by (a) the larger ionization parameter in the innermost NLR, and (b) mechanical heating.

A more realistic case might involve cylindrical symmetry, for example, a cylindrical NLR volume with radius 1 kpc and total height 3.4 kpc (the values appropriate for Mark 50; Falcke et al. 1998), where the axis of symmetry corresponds to the radio axis. No substantial difference from the spherically symmet-

ric models is expected as far as $\langle v \rangle$ is concerned, if similar assumptions about gas motions are made. However, the cylindrical symmetry case may give: (a) a larger CIV $\lambda 1549$ flux with respect to the spherically symmetric case and (b) a possibly broader CIV $\lambda 1549$ due to the pressure exerted by the jet, which could accelerate dense gas clumps. Mechanical heating may also provide a suitable mechanism for dust destruction. More sophisticated modelling (e. g. Steffen et al. 1997; Bicknell et al. 1998) is beyond the scope of this paper.

4. Results

4.1. The Intermediate Line Region: is it *præter necessitatem*?

Introduction of an additional (e.g. ILR) emitting region can be justified by the following (not mutually exclusive) circumstances: 1) spatial segregation (e.g. region associated with a jet) and/or 2) an abrupt discontinuity in physical properties (e.g. optical thickness or cloud instability at some distance). This is the physical statement of Occam's razor (*multipli-canda non sunt præter necessitatem*). The above circumstances describe the justification for the concept of distinct BLR and NLR regions where suppression of collisional lines yield different spectra. However “ILR” emission and coronal lines ($\langle v \rangle \approx 1 - 2 \times 10^3\text{ km s}^{-1}$) can be produced in the inner part of the NLR which, even if associated with an inner sheet adjacent to radio plasma, does not require introduction of a new distinct and discontinuous emitting region.

Part of the confusion over the identification of different line emitting components may have arisen from a difference in nomenclature. Wills et al. (1995) and Brotherton et al. (1994a,b) refer to the broader and narrower CIV components as very broad line (VBLR) and intermediate line (ILR) respectively. However they also inferred (Brotherton et al. 1994b) that the ILR properties (reverberation distance from continuum source, density, covering factor) are all similar to the standard NLR values. The ILR may be an “inner part of the NLR” but it is NLR and not BLR gas. Our models strengthen this view. The VBLR designation is also confusing because this name has already been applied to an even broader component sometimes seen in the HeII $\lambda 4686$ feature (Ferland et al. 1990; Marziani & Sulentic 1993).

4.2. BLR Implications

The model calculations support our two-component NLR-BLR interpretation of the CIV and H β profiles. Of course greater broad line profile complexity is sometimes observed, with double-peaked Balmer line profiles an extreme example. The relative strength and frequency of occurrence of multiple BLR components is not yet well established. However one interprets the narrower CIV feature, there is no justification for treating it as BLR gas. A number of recent studies involving the CIV BLR have analysed profile data without the benefit of subtracting any NLR component (e.g. Wills et al. 1993; Brotherton et al. 1994ab; Corbin & Francis 1994; Corbin & Boroson 1996).

Does it matter if an NLR component is subtracted from CIV? Our results suggest that the answer is a strong “yes”. The NLR component subtracted from CIV (in MS) represented 2-20% of the total flux in most cases. This flux was concentrated in the narrow peak of the line and therefore affected disproportionately determinations of the half maximum level of the broad line profile. The result of nonsubtraction yields line parameters surprisingly different from those obtained by MS. Figure 3 shows a comparison of CIV centroid line shifts (relative to [OIII]5007) for sources in common between MS and Corbin & Boroson (1996). A similar comparison also reveals that the CIV BLR profile width (FWHM) is measured, on average, 40% smaller when an NLR component is not subtracted. High ionization line BLR properties inferred from CIV, arguably the least confused HIL line, are dependent on whether or not an NLR is subtracted.

If an NLR component is subtracted, MS survey results suggest that: 1) radio-loud (RL) AGN show fundamentally different BLR geometry/kinematics from the radio quiet (RQ) majority, 2) in RQ-BLR CIV is blueshifted (up to 3000 km s $^{-1}$) with respect to the local rest frame while H β show small red and blue velocity shifts (up to 600 km s $^{-1}$) about that frame and 3) In RL-BLR CIV shows zero, or small red and blue (up to 1000 km s $^{-1}$), velocity excursions relative to the rest frame while H β shows larger predominantly red (but sometimes blue) shifts (up to 3000 km s $^{-1}$) relative to that frame. These effects must be tested with samples that cover a larger source luminosity range.

PM acknowledges financial support by Italian Ministry for University and Research (MURST) under grant Cofin98-02-32.

5. References

Antonucci, R. and Miller, J. 1985, *ApJ*, 297, 621

Baldwin, J. 1998, In proceedings of Emission Lines in Active Galaxies, eds. B. Peterson et al., ASP Conf. Ser., 113, 80

Bicknell, G. V., Dopita, M. A., Tsvetanov, Z. I., & Sutherland, R. S. 1998, *ApJ*, 495, 680

Brotherton, M. S., Wills, B. J., Steidel, Ch., & Sargent W. L. W., 1994a, *ApJ*, 423, 131

Brotherton, M. S., Wills, B. J., Francis, P. J., & Steidel, Ch. C. 1994b, *ApJ*, 430, 495

Caganoff, S., et al. 1991, *ApJ* 377, 9

Capetti, A., et al. 1999, MemSAIt, in press

Corbin, M. & Francis, P. 1994, *AJ*, 108, 2016

Corbin M., R., & Boroson, T. 1996, *ApJ Suppl*, 107, 69

De Robertis, M. M., & Osterbrock, D. E. 1986, *ApJ*, 301, 727

Falcke, H., Wilson, A. and Simpson, C. 1998, *ApJ*, 502, 199

Ferguson, J., Korista, K. and Ferland, G. 1997, *ApJ Suppl*, 110, 287

Ferland, G., Korista, K. and Peterson, B. 1990, *ApJ*, 363, L21

Ferland, G. J. 1996, Hazy: a Brief Introduction to CLOUDY, Univ. Kentucky, Dept. Phys. & Astron., internal report

Goad, M., & Koratkar, A. 1998, *ApJ* 495, 718

Heckmann, T. et al. 1995, *ApJ*, 452, 549

Kraemer, S., et al. 1994, *ApJ*, 435, 171

Kraemer, S., Crenshaw, D., Filippenko, A. and Peterson, B. 1998, *ApJ*, 499, 719

Kraemer, S., Ruiz, J. and Crenshaw, M. 1998, *ApJ*, 508, 232

Marziani, P. & Sulentic, J. W. 1993, *ApJ*, 409, 612

Marziani, P., Sulentic, J. W., Dultzin-Hacyan, D., Calvani, M. & Moles, M. 1996, *ApJ Suppl*, 104, 37 (MS)

Netzer, H., 1990, in Active Galactic Nuclei, Saas Fee Advanced Course 20, R.D. Blandford, H. Netzer, L. Woltjer (Berlin:Springer), p. 57

Steffen, W., Gomez, J. L., Raga, A. C., & Williams, R. J. R. 1997, *ApJ* 491, L73

Villar-Martin, M., Binette, L. and Fosbury, R. 1999, *A&A*, in press

Wills, B. et al. 1993, *ApJ*, 415, 563

Wills, B. J., Thompson, K. L., Han, M., Netzer, H., Wills, D., Baldwin, J. A., Ferland, G. J., Browne, I. W. A., & Brotherton, M. S. 1995, *ApJ* 447, 139

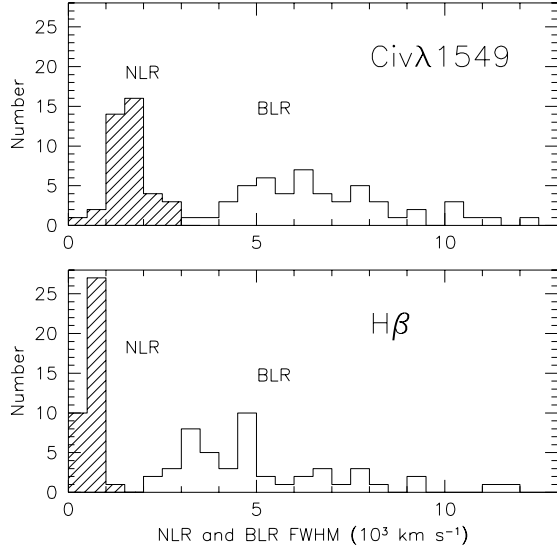


Fig. 1.— FWHM distributions for the broad and narrow components of CIV and H β . Data from the MS survey (Marziani et al. 1996).

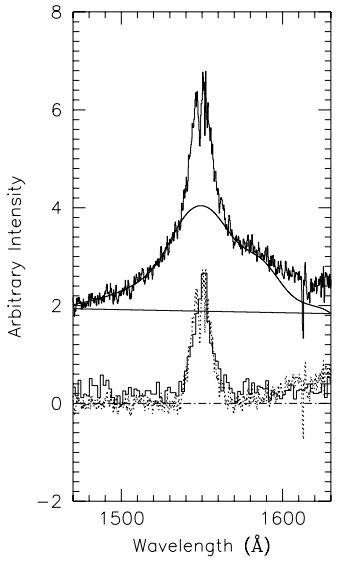


Fig. 2.— CIV λ 1549 profiles for: i) PG 2308+09 (upper) - smooth line shows fits to the BLR and continuum components and ii) NGC 5643 EELR (lower) - scaled and without continuum subtraction. NLR component of PG2308+09 superposed (dotted). Note the similar profile widths.

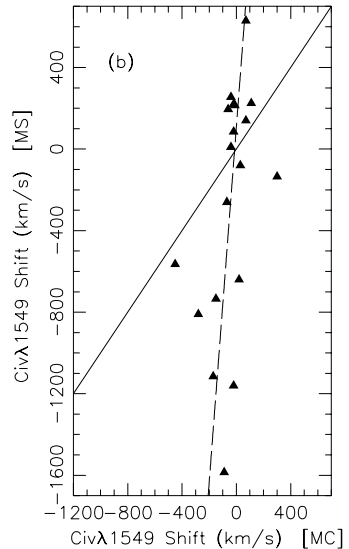


Fig. 3.— CIV BLR profile shift measurements (at FWHM level) for sources in common between the MS survey and Corbin & Boroson (1996) (MC). Dashed line is an unweighted least squares fit and the thin line the locus of equal shifts. MC measures are consistent with no shift within the errors (± 200 km s $^{-1}$).

TABLE 1
MODEL COMPUTATIONS

Model (1)	$\log(n_0)$ (cm $^{-3}$) (2)	m (3)	r_s ¹ (pc) (4)	$\langle v \rangle$ $H\beta_{NC}$ (km s $^{-1}$) (5)	$\langle v \rangle$ [OIII] $\lambda 5007$ (km s $^{-1}$) (6)	$\langle v \rangle$ [Fe VII] $\lambda 6087$ (km s $^{-1}$) (7)	$\langle v \rangle$ CIV $\lambda 1549_{NC}$ ² (km s $^{-1}$) (8)
1	8	$\frac{7}{18}$	10	490	450	1030	1370
2	7	$\frac{11}{18}$	10	420	310	950	1250
3	8	$\frac{7}{18}$	1	720	440	1160	2680
4	8	$\frac{13}{18}$	10	370	340	980	1380
5	7	$\frac{13}{18}$	10	370	490	910	1210
6	8	$\frac{13}{18}$	1	380	330	1020	1450
7	7	$\frac{13}{18}$	1	360	520	925	1950

¹Scale factor for mechanical heating, assumed to decrease exponentially from r_0 (see text).

²Width of single line.